



Contents lists available at ScienceDirect

## Journal of King Saud University - Science

journal homepage: [www.sciencedirect.com](http://www.sciencedirect.com)

# Particulate matter concentrations around natural gas-fired power plants and their associated health impact assessment

Mustafizur Rahman<sup>a,b</sup>, Kamrul Hasan<sup>a,f</sup>, Md. Abu Bakar Siddique<sup>c</sup>, Balram Ambade<sup>d</sup>,  
Md. Alamgir Hussain<sup>b,e</sup>, Mohammed Abdus Salam<sup>a,\*</sup>, Salman Tariq<sup>g,h</sup>, Muhammad Ibrahim<sup>i</sup>

<sup>a</sup> Department of Environmental Science and Disaster Management (ESDM), Noakhali Science and Technology University (NSTU), Noakhali 3814, Bangladesh

<sup>b</sup> Department of Quality, Environment, Health, and Safety (QEHS), United Engineering and Power Services Limited (UEPSL), United Group, United City, Madani Avenue, Dhaka 1212, Bangladesh

<sup>c</sup> Institute of National Analytical Research and Service (INARS), Bangladesh Council of Scientific and Industrial Research (BCSIR), Dhanmondi, Dhaka 1205, Bangladesh

<sup>d</sup> Department of Chemistry, National Institute of Technology, Jamshedpur 831014, Jharkhand, India

<sup>e</sup> Advanced Engineering Management (AEM), Department of Industrial and Production Engineering, Bangladesh University of Engineering and Technology (BUET), Dhaka 1000, Bangladesh

<sup>f</sup> Department of Environmental Science, Gazi University, Turkey

<sup>g</sup> Department of Space Science, University of the Punjab, Lahore, Pakistan

<sup>h</sup> Remote Sensing, GIS and Climatic Research Lab (National Center of GIS and Space Applications), Centre for Remote Sensing, University of the Punjab, Lahore, Pakistan

<sup>i</sup> Department of Environmental Sciences, Government College University Faisalabad, Pakistan

## ARTICLE INFO

## Keywords:

Gas-fired power plants

Particulates

Air quality

ARIMA, ANN, and ETS forecasting

Health impact assessment

## ABSTRACT

The quantification and prediction of particulate matter (PM) concentrations in the air are essential due to their negative impacts on human health and the environment. This study quantified PM concentrations and associated health effects at four natural gas-based power plants in Bangladesh. The measurement of PM<sub>2.5</sub> and PM<sub>10</sub> using the respirable dust samplers APS-113NL and APS-113BL, respectively from the year of 2015 to 2021 revealed that the concentration of both types of particles fluctuated over the years. The highest recorded levels of particles were in 2019, with PM<sub>2.5</sub> at 126 µg/m<sup>3</sup> and PM<sub>10</sub> at 283 µg/m<sup>3</sup> and the lowest recorded levels of particles were in 2017, with PM<sub>2.5</sub> at 76.3 µg/m<sup>3</sup> and PM<sub>10</sub> at 203.3 µg/m<sup>3</sup>. In 2021, PM<sub>2.5</sub> and PM<sub>10</sub> concentrations were 88.5 and 225 µg/m<sup>3</sup>, respectively, lower than in the past two years. Statistical modeling assessed atmospheric contaminants analyzed time series data, and projected air quality. ARIMA, ETS, and ANN modeling methods have been used to predict the monthly average of PM<sub>2.5</sub> and PM<sub>10</sub> concentrations. RMSE, MAPE, MASE, and MAE have been utilized for model orders, time series analysis, and forecasting validation. There is a significant variation between the forecasting models and forecasts for average PM<sub>2.5</sub> and PM<sub>10</sub> concentrations in natural gas-fired power plants from 2022 to 2024. This study also conducted a face-to-face interview with over 100 employees using a structured questionnaire to assess the health effects they are facing due to poor air quality in the power generation complex and found that 2 and 13 % of employees had respiratory and skin issues, respectively. Nonetheless, regular health checks, air filtration, and renewable energy consumption may benefit residents and the environment.

## 1. Introduction

Industrial, social, and economic progress requires access to

electricity, and fossil fuel resources play a major role in the production of electricity long into the 21st century, but their emissions also have a significant negative impact on human health (Markandya and

**Abbreviations:** AIC, Akaike information criterion; AQI, Air Quality Index; ANN, Artificial Neural Network; ARIMA, Auto-Regressive Integrated Moving Average; ADF, Augmented Dickey-Fuller; BIC, Bayesian Information Criterion; EPA, Environmental Protection Agency; ETS, Error Trend Seasonal; MAE, Mean Absolute Error; MAPE, Mean Absolute Percentage Error; MASE, Mean Absolute Scaled Error; MW, Megawatt; NG, Natural Gas; PM, Particulate Matter; RMSE, Root Mean Squared Error.

\* Corresponding author.

E-mail addresses: [mustafiz731@gmail.com](mailto:mustafiz731@gmail.com) (M. Rahman), [masalam.esdm@nstu.edu.bd](mailto:masalam.esdm@nstu.edu.bd) (M.A. Salam).

<https://doi.org/10.1016/j.jksus.2024.103270>

Received 7 February 2024; Received in revised form 19 May 2024; Accepted 21 May 2024

Available online 23 May 2024

1018-3647/© 2024 The Authors. Published by Elsevier B.V. on behalf of King Saud University. This is an open access article under the CC BY-NC-ND license (<http://creativecommons.org/licenses/by-nc-nd/4.0/>).

Wilkinson, 2007). In 2013, the world used  $532.9 \times 10^{18}$  J equivalent of fossil fuel energy, and in 2018, world energy consumption increased remarkably. In 2020, global energy demand was significantly higher ( $654 \times 10^{18}$  J) compared to 2000 ( $428 \times 10^{18}$  J). Similarly, the projected energy requirement in 2035 will almost double ( $812 \times 10^{18}$  J) that of 2008 (Rashid and Joardder, 2022). Global power consumption is predicted to double by 2050 (Holecek et al., 2022; Sokulski et al., 2022). During COVID-19, electricity generation from coal, natural gas, and other facilities declined by up to 35, 25, and 20 percent, respectively, while the percentage of renewable energy climbed by up to 9 % (Ghenai and Bettayeb, 2021) at the same time studies also observed reductions in PM emissions ranging from 30 % to 50 % in countries like China, India, and the United States (Vultaggio et al., 2020). The impact on PM emissions varied depending on the specific fuel-switching practices and emission control technologies employed. Some studies showed slight reductions in PM from gas plants, while others observed little change (Gu et al., 2021). Regardless, the global decrease in PM during lockdowns led to significant air quality improvements (Vultaggio et al., 2020).

By Oct 2019, Bangladesh's power grid was booming with 22,562 MW capacity (including captive and renewable energy) (Islam et al., 2021; PSMP, 2016). Access to electricity in Bangladesh is growing rapidly, with almost 95 % of the population having access to electricity, and a total of 3,493 MW of electricity generating capacity was added to the national grid during the 2018–19 fiscal year. This brought the total generating capacity up to 18,961 MW, and the yearly increment of generation capacity was 18.86 %. Bangladesh Power Development Board (BPDB) contributed 2,563 MW (including IPPs and power import) of electricity from this new capacity addition. (Islam and Khan, 2017) The majority of electricity in Bangladesh is generated from fossil fuel combustion, heavy fuel oil combustion (3 %), burning of natural gas (62.9 %) and coal (5 %), and 3.3 % from renewable sources (Anam and Husnain-Al-Bustam, 2011). Bangladesh has the ambition to become a high-income country by 2041, and energy and power infrastructure development pursue quantity and quality to realize long-term economic expansion (PSMP, 2016). It is a big challenge for Bangladesh due to the high electricity demand of the population of 158.9 million (BBS et al., 2017). In addition, electricity generation from fossil fuel sources has proven to be a significant source of air pollution, including in Bangladesh (Rahman et al., 2024). Bangladesh is a developing country facing the worst air pollution issues due to massive development work and industrial activities (Begum et al., 2014a; Shahriar et al., 2020). Human exploitation of resources, fossil fuel burning, and development activities cause greenhouse gas (GHG) emissions, particulate matter (PM) intrusion, and environmental degradation (Ghosh, 2002). Many pollutants, such as Carbon Dioxide (CO<sub>2</sub>), Nitrous oxide (N<sub>2</sub>O), PM<sub>2.5</sub>, and PM<sub>10</sub> in the air are emitted from different sources like the power generation sector and pollute the environment (Bai et al., 2018).

However, advancements in energy market policies, such as cap-and-trade programs, offer promising solutions for emissions reduction from gas-fired power plants. These programs can contribute significantly and have been shown to improve social welfare (Dimitriadis et al., 2023). It is also well known that energy is crucial for poverty reduction, economic growth, and infrastructure development. However, the pollution caused by electricity generation, particularly GHGs and PM, poses significant challenges. These pollutants have adverse effects on living organisms and contribute to air pollution worldwide (Cellura et al., 2018; Ibe et al., 2020; Shin et al., 2022a). PM<sub>10</sub> and PM<sub>2.5</sub> are so small that they can be inhaled, penetrate the lungs, and cause serious health problems like asthma, pneumonia, lung disorder, etc. (Begum et al., 2014b; Woodward et al., 2014). It is also a major cause of early death and illness around the world. A study on the Global Burden of Disease found that in 2019, outdoor air pollution was responsible for an estimated 6.67 million premature deaths (Cheng et al., 2007). PM emissions from fossil fuel-fired power plants are linked to fuel combustion, engine operation, maintenance process, and running hours and, therefore, can be related

to the amount of generated energy (Abdul Jameel et al., 2016). Globally, approximately 60 % of electricity is generated from burning fossil fuels, mostly coal and natural gas, and contributes to atmospheric pollution, which poses a threat to health (Al-Amin and Sahabuddin, 2023). Exposure pathways for air pollutants include inhalation of dust and gases and ingesting contaminated food and water (Qu et al., 2012). The PM was chosen as a focus due to its known harmful effects on human health and the environment. In addition, forecasts of PM concentrations in power complexes are necessary to plan for health concerns.

Auto-Regressive Integrated Moving Average (ARIMA), Error Trend Seasonal (ETS), and Artificial Neural Network (ANN) models each offer specific advantages depending on the desired forecast horizon and data complexity (Kim et al., 2022). ARIMA excels in capturing temporal dependencies for short-term predictions, while ETS efficiently handles trends and seasonality for medium-term needs (Thabani et al., 2019). ANN boasts flexibility and potential for superior accuracy in capturing intricate relationships for long-term forecasts but requires large datasets and significant computational resources (Eğrioğlu et al., 2008; Radojević et al., 2013). Choosing the most suitable model depends on data availability, interpretability needs, and computational resources. Comparing model performance and considering hybrid approaches utilizing the strengths of each can be beneficial (Kim et al., 2022). This study aims to forecast PM<sub>2.5</sub> and PM<sub>10</sub> concentrations in power generation complexes in Bangladesh to assess their potential health impacts. By employing time series analysis methods like ARIMA, ETS, and ANN, we aim to develop accurate forecasts. These forecasts will be crucial for regulatory planning to control PM emissions and protect public health in Bangladesh.

## 2. Materials and methods

### 2.1. Study area

This study was carried out over four natural gas-based power plants situated in four different districts in Bangladesh. For air sampling, one representative location was chosen from each of the power plants located at Tangail (24°19' N and 89°55' E), Chittagong (22°17' N and 91°46' E), Feni (23°1' N and 91°22' E), and Narshingdi (23°55' N and 90°41' E) districts (Fig. 1). These areas are home to several industries, including natural gas-fired power plants and manufacturing facilities, which contribute to atmospheric pollution. According to BBS 2020, the population density of these regions is 1500, 32008, 2200, and 1056 km<sup>2</sup>, with many residents working in these industries. The study area is located in a region with a temperate climate and experiences seasonal variations in weather conditions (Chowdhury et al., 2022).

### 2.2. Data collection and analysis

The study utilized two main data sets about Particulate Matter (PM) and employee health surveys. Data regarding PM<sub>2.5</sub> and PM<sub>10</sub> were collected month-wise from January 2015 to December 2021 using respirable dust samplers APS-113NL for PM<sub>2.5</sub> and APS-113BL for PM<sub>10</sub> from the ambient air near selected engine-based natural gas-fired power plants.

In developing our machine learning models for PM<sub>2.5</sub> and PM<sub>10</sub> concentration forecasting, we utilized this collected historical data from 2015 to 2021. To ensure model development and evaluation, we employed a training–testing split. Data from 2015 to 2019 (roughly 71.43 % of the total data) served as the training set, where the models learned the patterns within the historical information. The remaining data from 2020 to 2021 (approximately 28.57 %) functioned as the testing set, allowing an unbiased assessment of the model's generalizability and ability to predict unseen data. Finally, after training and evaluation, we leveraged the models to forecast PM<sub>2.5</sub> and PM<sub>10</sub> concentrations for the years 2022, 2023, and 2024. To list employee health problems, face-to-face interviews were conducted using a representative

### Study Area Map

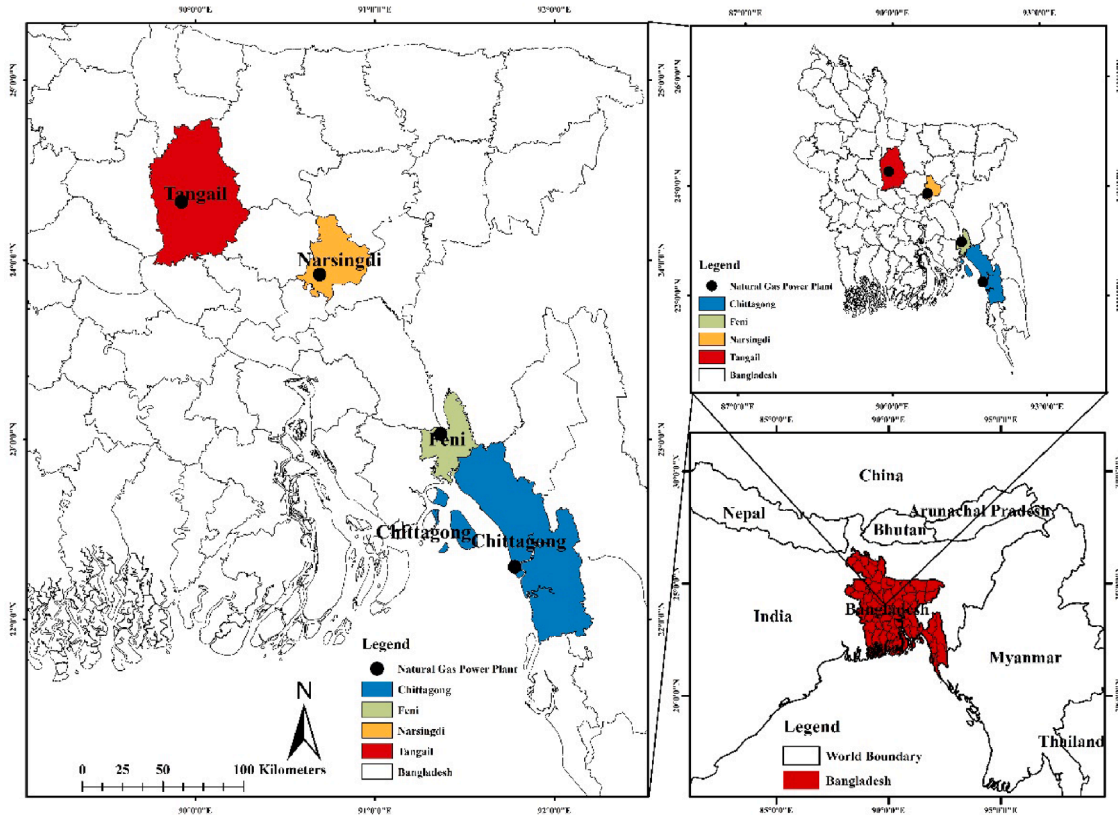


Fig. 1. Natural gas-fired power plant locations selected for data collection.

and structured questionnaire about health issues among the randomly selected 100 employees who have been working in the electricity generation plant for over two years. The analysis methods of this study are entirely based on the information extracted from four natural gas-fired power plants (72 MW Chittagong, 22 MW Feni, 22 MW Narshingdi, and 22 MW Tangail). Air Quality Index (AQI) values and PM<sub>2.5</sub> and PM<sub>10</sub> were collected from the previous documents of each power plant. The AQI value was processed to determine PM<sub>2.5</sub> and PM<sub>10</sub> values following equations (1) and (2), respectively, and the breakpoint Table (Table 1), all prescribed by environmental protection agencies (EPAs) (Cheng et al., 2007).

$$I_{PM2.5} = \left\{ \frac{(I_{high} - I_{low})}{(C_{high} - C_{low})} \right\} \times (AQI - C_{low}) + I_{low} \tag{1}$$

$$I_{PM10} = \left\{ \frac{(I_{high} - I_{low})}{(C_{high} - C_{low})} \right\} \times (AQI - C_{low}) + I_{low} \tag{2}$$

where  $I_{PM2.5}$  = Particulate Matter 2.5 Emission ( $\mu\text{g}/\text{m}^3$ ),  $I_{PM10}$  = Particulate Matter 10 Emission ( $\mu\text{g}/\text{m}^3$ ),  $I_{high}$  = Index breakpoint corresponding to  $C_{high}$ ,  $I_{low}$  = Index breakpoint corresponding to  $C_{low}$ ,  $C_{high}$  = The concentration breakpoint  $\geq C$ ,  $C_{low}$  = The concentration breakpoint  $\leq C$ .

**Table 1**  
Air quality index (AQI) and breakpoint prescribed by environmental protection agencies.

AQI	Level of health concern	PM <sub>2.5</sub> ( $\mu\text{g}/\text{m}^3$ )	PM <sub>10</sub> ( $\mu\text{g}/\text{m}^3$ )
0–50	Good	0–15.4	0–54
51–100	Moderate	15.5–40.4	55–154
101–150	Unhealthy for sensitive group	40.5–65.4	155–254
151–200	Unhealthy	65.5–150.4	255–354
201–300	Very unhealthy	150.5–250.4	355–424
301–400	Hazardous	250.5–350.4	425–504
401–500	Very hazardous	350.5–500.4	505–604

To assess health hazards due to PM, the forecasted values were compared with the EPA’s breakpoint AQI value. Finally, data were recorded and analyzed using Rstudio and Microsoft Excel, and a study area map was prepared using ArcGIS software. ARIMA, ETS, and ANN models were used to analyze and forecast PM<sub>2.5</sub> and PM<sub>10</sub> concentrations in specific power generation plants. The analysis involved in this article has run on the R-4.0.5 workstation. This study prepared its R routines that suited the procedure adopted. Natural gas power plant data from 2015 to 2021 were analyzed using ARIMA, ETS, and ANN models for time series analysis and forecasting. While the ARIMA model is generally considered computationally efficient compared to some other time series forecasting methods, the actual computation time can vary depending on factors like data size and model complexity (p, d, q values). In larger datasets or with more complex models, computation time may increase (Hyndman and Khandakar, 2008).

#### 2.3. Auto-Regressive Integrated Moving average (ARIMA)

Box Jenkins was used to analyze the data and forecast emissions in this study. Time series can be stationary or non-stationary, and this technique fits neatly into the category of the linear model. Box-Jenkins methods are helpful in forecasting because they include Autoregressive (AR) models, integrated (I) models, and Moving Average (MA) models. The Box-Jenkins methodology requires four steps to obtain the model: data preparation, model selection, estimation, and forecasting. A model is then employed as a prediction tool. After data collection, we first determined whether the data were part of a stationary or non-stationary time series. To identify these data, we used the augmented Dickey-Fuller (ADF) test. The differencing methodology may be used to make a time series stationary if it does not exhibit covariance stationary. The ARIMA (p, d, q) model is created by applying the ARMA (p, q) model to stationary differenced time series, where d is the order of differencing. We

used the ADF test after the difference, which reveals the stationary time series. One approach for identifying trends in the data is the autocorrelation function. The autocorrelation function informs users of the correlation between points separated by different time lags. Given a sample  $Y_0, Y_1, \dots, Y_{T-1}$  of  $T$  observations, we define the sample autocorrelation function to be the sequence of values,

$$r_\tau = C_\tau / C_0, \tau = 0, 1, \dots, T - 1 \tag{3}$$

The partial autocorrelation function (PACF) in time series analysis provides the partial correlation of a time series with its own lagged values while controlling for the importance of the time series at all shorter lags. The sample partial autocorrelation  $P_\tau$  at lag  $\tau$  is simply the correlation between the two sets of residuals obtained from regressing the elements  $Y_t$  and  $Y_{t-\tau}$  on the set of intervening values  $Y_1, Y_2, \dots, Y_{t-\tau+1}$ . The Akaike information criterion (AIC) compares statistical model quality. The "best" model will be characterized by which doesn't fit either too well or too poorly. AIC is usually calculated with the software. The basic formula is defined as follows.

$$AIC = -2(\log - likelihood) + 2K \tag{4}$$

Log-likelihood is a method for measuring the model's fit, where  $K$  is the total parameter count (model variables plus intercept). The bigger the number, the better the fit. This is usually obtained from statistical output. In statistics, the Bayesian Information Criterion (BIC) may be a criterion for model selection among a finite set of models; the model with rock-bottom BIC is preferred. It is based partly on the likelihood function, and it is closely associated with the AIC. The solution proposed by BIC and AIC is to include a penalty term for the number of parameters in the model.

2.4. Forecasting with error Trend seasonal (ETS) model

ETS point forecasting is obtained from the models by iterating the equations for

$$t = T + 1, \dots, T + h \text{ and setting all } \epsilon_t = 0 \text{ for } t > T \tag{5}$$

Therefore,

$$\bar{y}_{T+1|T} = \ell T + bT \tag{6}$$

Similarly,

$$\begin{aligned} y_{T+2} &= (\ell T + 1 + bT + 1)(1 + \epsilon T + 2) \\ &= [(\ell T + bT)(1 + \alpha \epsilon T + 1) + bT + \beta(\ell T + bT)\epsilon T \\ &\quad + 1](1 + \epsilon T + 2) \end{aligned} \tag{7}$$

Therefore,

$$\bar{y}_{T+2|T} = \ell T + 2bT \tag{8}$$

These forecasts are identical to the estimates from the model ETS as well as Holt's linear method (A, A, N). As a result, the point forecasts obtained using the technique and the two models that form its foundation are the same (assuming that the same parameter values are used). ETS point forecasts are equivalent to the forecast distributions' medians. The forecast distributions are normal for models with only additive components, so the medians and means are equal. The point forecasts and the standards of the forecast distributions will not be the same for ETS models with multiplicative errors or with multiplicative seasonality.

2.4.1. ETS model prediction intervals

ETS models can generate prediction intervals, but additive and multiplicative models have different prediction intervals. A prediction interval for the majority of ETS models is written as

$$\bar{y}_T + h|T \pm c\sigma_h \tag{9}$$

Where forecasting method (A, N, A),  $c$  depends on the coverage probability, and  $\sigma_h^2$  is the forecast variance.

$$\sigma_h^2 = \sigma^2 [1 + \alpha^2(h - 1) + \gamma k(2\alpha + \gamma)] \tag{10}$$

2.5. Forecasting with Artificial neural network (ANN) model

ANN is a data processing system that takes inspiration from the human brain and uses a network of many tiny processors to process data. In these networks, a programmed data structure acts like a neuron. A training algorithm is used to train a network that connects all neurons. Artificial neurons have two inputs and outputs. There are two states for every neuron: training and acting. A neuron learns the appropriate outputs for a particular input during the training phase. When information is defined for the neuron in the active state, it produces the proper output based on the training. While the hidden layer in the ANN model for PM concentration forecasting doesn't directly transmit raw data, it plays a vital role in uncovering complex patterns. It acts as a feature extractor, using non-linear activation functions to transform the lagged PM concentration values (input data) and identify underlying trends or relationships. This processed information represents a higher-level abstraction, capturing the essential features most relevant for prediction. The hidden layer then transmits this processed representation, not the raw data itself, to the output layer. Finally, the output layer leverages this learned representation to make the final prediction of future PM concentrations. In essence, the hidden layer acts as a crucial bridge, transforming the raw data into a form that the output layer uses to generate accurate forecasts.

This type of network is referred to as a multilayer feed-forward network, and it is characterized by the fact that each layer of nodes receives inputs from the layers that came before it. The inputs of the nodes in one layer come from the outputs of the nodes in the previous layer. Weighted linear combination combines each node's inputs. A nonlinear function modifies the output result.

If the inputs into hidden neuron  $j$  in Fig. 2 are combined linearly to give,

$$Z_j = b_j + \sum_{i=1}^4 W_{i,j} X_i \tag{11}$$

This is then adjusted using a nonlinear function, such as a sigmoid in the hidden layer so that it can act as input for the following layer. This reduces the impact of extreme input values, making the network somewhat resilient to outliers.

$$S(z) = \frac{1}{1 + e^{-z}} \tag{12}$$

The values of the parameters  $b_1, b_2, b_3$ , and  $W_{1,1}, \dots, W_{4,3}$  are "learned" from the data. Limits are typically placed on the weight values to prevent them from becoming excessive. The value 0.1 is frequently used for the "decay parameter," which is the parameter that controls the

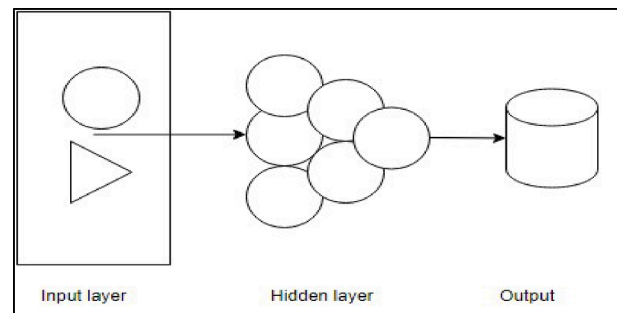


Fig. 2. An artificial neural network (ANN) with two inputs and one hidden layer with hidden neurons.

weight restrictions. The weights start with random values, and then those values are modified based on the data that has been observed. So, the predictions made by a neural network have a bit of a random element to them. The network is usually trained more than once using different random starting points, the results are averaged, and hidden layers and nodes are defined in advance.

2.5.1. Neural network autoregression (NNAR)

When using a neural network with time series data, the lag values of the time series are utilized as inputs. This study used lagged values in a linear autoregression model, called a neural network autoregression or NNAR model. This study considered feed-forward networks with one hidden layer and used the notation NNAR (*p*, *k*) to indicate there are *p*-lagged inputs and *k* nodes in the hidden layer. With seasonal data, including the most recent data from the same season as inputs is helpful, and the NNAR (*p*, *P*, *k*) model fits the function. If *p* and *P* are not given, a random value will be chosen for them. The default for non-seasonal time series is the optimum number of lags for a linear AR(*p*) model. *P* is set to 1 by default for seasonal time series, and *p* is selected from the best linear model fit to the data with seasonal adjustments. If *k* is left unspecified, the default value is  $k = (p + P + 1)/2$  (rounded to the nearest integer). When it comes to making predictions, the network is used iteratively. This study simply used the available historical inputs to forecast one step. The one-step prediction was used as input to predict two steps with the previous data. This procedure continues until all the needed projections are calculated.

2.5.2. Prediction intervals

The foundation of neural networks is not a well-defined stochastic model; as a consequence, calculating prediction intervals for the resulting projections is difficult. However, through simulation, we have calculated prediction intervals where future sample pathways are produced using bootstrapped residuals. The neural network fitted to the PM data can be written as

$$y_t = f(y_{t-1}) + \epsilon_t \tag{13}$$

where  $y_{t-1} = (y_{t-1}, y_{t-2}, \dots, y_{t-10})^T$  is a vector containing lagged values of the series, and *f* is a neural network with six hidden nodes in a single layer. The error series {*εt*} is assumed to be homoscedastic (maybe a normal distribution). The ability to simulate future sample paths of this model repeatedly by selecting a value at random for *εt*, either from a normal distribution or by resampling the historical values.

So, if  $\epsilon_{T+1}$  is a random draw from the distribution of errors at time *T* + 1, then  $y_{T+1} = f(y_T) + \epsilon_{T+1}$  is one possible draw from the forecast distribution for *yT* + 1.

Setting,  $y_{T+1} = (y_{T+1}, y_T, \dots, y_{T-8})^T$ , we can then repeat the process to get  $y_{T+2} = f(y_{T+1}) + \epsilon_{T+2}$ .

In this manner, this may repeatedly simulate a future sample route. This study gains knowledge of the distribution for all future values by continually forging sample routes based on the fitted neural network.

3. Results and discussion

3.1. Particulate matter (PM) concentration scenario in natural gas-fired power plant

Table 2 shows the concentration of PM<sub>2.5</sub> and PM<sub>10</sub> in the natural gas burning in 4 storks internal combustion engines in four power plants located in Chittagong, Feni, Narshingdi, and Tangail districts of Bangladesh, generating a yearly capacity of 1208.88 GW. PM concentrations in power plants depend on operation, fuel burning, and air filtering. Wartsila and Rolls Royce engines ensure rich burn to avoid carbon monoxide and PM emissions. This study covered four natural gas power plants in different locations to analyze PM<sub>2.5</sub> and PM<sub>10</sub> data from 2015 to 2021 and forecast. The concentration of PM in the atmosphere

Table 2  
Particulate matter concentration status in natural gas-based power plants.

Year	*EPA's standard (µg/m <sup>3</sup> )		PM <sub>2.5</sub> µg/m <sup>3</sup>	PM <sub>10</sub> µg/m <sup>3</sup>
	PM <sub>2.5</sub>	PM <sub>10</sub>		
2015	12-15	>150	86.8	229.3
2016			95.4	211
2017			76.3	203.3
2018			83.0	207.8
2019			126	283
2020			122.6	279
2021			88.5	225

\*U.S. Environmental Protection Agency (Minh et al., 2021).

has increased day by day as a result of fuel burning and steady emissions from fossil fuel-burning power plants without filtering, construction work, or other development activities (Shin et al., 2022b). PM emissions are not directly from fuel burning and indicate ambient PM concentrations in the electricity generation area. According to EPA standards, monitored PM concentrations are unhealthy in all fossil fuel-burning power plants. PM<sub>2.5</sub> and PM<sub>10</sub> concentrations in selected power generation complexes have fluctuated over the past seven years, and the highest average PM<sub>2.5</sub> concentration was recorded in 2020, at 122.6 µg/m<sup>3</sup>. The lowest average PM<sub>2.5</sub> concentration was recorded in 2017, at 76.3 µg/m<sup>3</sup>. PM<sub>10</sub> concentrations generally followed a similar trend to PM<sub>2.5</sub> concentrations, and both PM<sub>2.5</sub> and PM<sub>10</sub> concentrations exceeded the EPA's standard in all years measured (Table 2).

3.2. Forecasting of PM<sub>2.5</sub> and PM<sub>10</sub> using ARIMA, ETS, and ANN models

In time series forecasting, ensuring the data is stationary (meaning its statistical properties remain constant over time) is crucial for obtaining reliable predictions. The ADF test is a common tool used to assess stationarity. As shown in Table 3, the ADF test results for PM<sub>2.5</sub> and PM<sub>10</sub> both have p-values less than 0.05 (a commonly used significance level) and negative test statistics, indicating a rejection of the null hypothesis of a unit root (non-stationarity) at the chosen significance level. The p-value is less than 0.05 for both variables, a commonly used statistical significance threshold. This further supports the conclusion of stationarity. The lag order is 3 for both PM<sub>2.5</sub> and PM<sub>10</sub>, indicating that the model used to perform the ADF test included 3 lags of the differenced data (Table 3). This shows we can reject the null hypothesis of non-stationarity, and both variables are likely stationary. With stationary data, we can proceed more confidently to our chosen forecasting model.

In this analysis of PM<sub>2.5</sub> and PM<sub>10</sub> concentration forecasting, ARIMA models emerged as a potentially better solution compared to ETS models based on AIC and BIC criteria. For PM<sub>2.5</sub>, an ARIMA (1,0,0) (1,1,0) [12] model captured the influence of the previous month's value (positive coefficient) along with a seasonal effect (negative coefficient). PM<sub>10</sub> also exhibited a seasonal pattern, but its ARIMA model ARIMA (1,0,0) (2,1,0) [12] included two seasonal autoregressive terms, suggesting a more complex seasonal influence. Overall, the importance of the seasonal component was evident in both PM<sub>2.5</sub> and PM<sub>10</sub>, while automated ARIMA models provided a better fit based on the chosen information criteria. These methods produce better prediction plots, and Fig. 4 demonstrates how accurate the predicted value was. We observed the data from 2015, 2016, 2017, and 2018 using the ARIMA model, and then we forecasted the data for 2019, 2020, and 2021. Even though we were aware of the data from 2019, 2020, and 2021, the mean absolute scaled error (MASE) value for PM<sub>2.5</sub> and PM<sub>10</sub> was MASE < 1, which

Table 3  
Data summary of unit root tests for PM<sub>2.5</sub> and PM<sub>10</sub>.

Variable	ADF test	Lag order	P-value	Alternative hypothesis
PM <sub>2.5</sub>	-3.9076	3	0.02018	Stationary
PM <sub>10</sub>	-3.9126	3	0.0212	Stationary

indicates the model does not need improvement and model is exactly as good (Wang and Lu, 2018). It is possible to say, based on a rule of thumb, lower Root mean squared error (RMSE) values, demonstrate that the model can predict the data accurately. Similarly, the ETS models for PM<sub>2.5</sub> and PM<sub>10</sub> employed additive errors and additive trend components. ETS (M, N, M), ETS (A, N, A), and NNAR (1,1,2) [12] were used for PM<sub>2.5</sub> and PM<sub>10</sub> series, which gives a better prediction plot. We observed the data as before observed for the ARIMA model from 2015, 2016, 2017, and 2018 using the ETS and ANN model, and then we forecasted the data for 2019, 2020, and 2021 (Table 4). The ANN model summary suggests it's not just a single model, but an ensemble of 20 similar ANNs with 2 hidden layers, each containing 2 neurons. These networks likely have slightly different weights leading to a more robust prediction. ANN model also has the total number of trainable parameters (weights and biases) in each network within the ensemble (2 neurons in the first layer \* 2 neurons in the second layer + biases = 9). The final layer of each network uses linear activation, meaning the output is a direct linear combination of the weighted inputs from the previous layer. However, the mean absolute error (MAE) of PM<sub>2.5</sub> from the ANN model was closer to zero than PM<sub>2.5</sub> from the ETS model, and PM<sub>10</sub> from the ETS model was closer to zero than PM<sub>10</sub> from the ANN model, which indicates PM<sub>2.5</sub> from the ANN model, and PM<sub>10</sub> from ETS model is more accurate than PM<sub>2.5</sub> from ETS and PM<sub>10</sub> from ANN model respectively (Eğrioğlu et al., 2008). According to the RMSE, MAE, MAPE (Mean absolute percentage error), and MASE values projected by the ARIMA, ETS, and ANN models, the expected value for PM concentration in natural gas-fueled power plant areas in 2022, 2023, and 2024 are accurate, and the model used for forecasting worked well. Table 4 compares the forecasts of ARIMA, ETS, and ANN models for PM<sub>2.5</sub> and PM<sub>10</sub> concentrations in the study area and shows the predicted concentrations for January to December in 2022, 2023, and 2024.

In Fig. 3, the x-axis of the graphs is time, ranging from 2015 to 2025. The y-axis is PM<sub>2.5</sub> or PM<sub>10</sub> concentration, measured in micrograms per cubic meter (µg/m<sup>3</sup>). The forecasts from the four models are shown as lines on the graphs. The solid line is the forecast, and the shaded area around the line represents the uncertainty of the forecast. The wider the shaded area, the less certain the forecast is. All three models predict that PM<sub>2.5</sub> and PM<sub>10</sub> concentrations will be highest in the winter months (December to February) and lowest in the summer months (June to August) (Fig. 3). The ARIMA model generally predicts the highest

concentrations of PM<sub>2.5</sub> and PM<sub>10</sub>, followed by the ETS model and then the ANN model. The ETS model tends to predict the most stable concentrations of PM<sub>2.5</sub> and PM<sub>10</sub> throughout the year, with less variation between months. The ANN model tends to predict the most volatile concentrations of PM<sub>2.5</sub> and PM<sub>10</sub>, with the most variation between months.

### 3.3. Accuracy between the observed value and the predicted value of PM<sub>2.5</sub> and PM<sub>10</sub>

Data on PM concentrations used to train ARIMA, ETS, and ANN models for modeling time series. The plots demonstrate that an ARIMA, ETS, or ANN model can be used to explain the observed time series. Fig. 4 displays, however, the degree of accuracy by the predicted value. To calculate the accuracy rate, we observed the data for 2015 to 2019 and forecasted data for 2020 and 2021. Though we knew the data for 2020 and 2021 (Fig. 4), the accuracy rate for PM<sub>2.5</sub> and PM<sub>10</sub> was good enough for the black line (Fig. 4), indicating observation, and the blue line for prediction.

Table 5 compares the performance of three different models named ARIMA, ETS, and ANN for predicting the concentration of two pollutants, PM<sub>2.5</sub> and PM<sub>10</sub>. It uses four different error measures RMSE, MAE, MAPE, and MASE, and a lower value indicates better performance. Overall, ANN and ARIMA seem to have comparable performance for PM<sub>2.5</sub> prediction based on RMSE and MAE. Both have very similar values. MAPE is slightly higher for ANN, while MASE is slightly lower. For PM<sub>10</sub> prediction, ANN might perform slightly worse than ARIMA based on RMSE and MAE. The difference is small though. MAPE is again slightly higher for ANN, while MASE is comparable. ETS seems to perform worse than both ARIMA and ANN for both pollutants based on all error measures. It has higher values for RMSE, MAE, MAPE, and MASE for both PM<sub>2.5</sub> and PM<sub>10</sub>. MAPE greater than 10 % but less than 25 % was found in ARIMA, ETS, and ANN models for PM<sub>10</sub> and indicates low but acceptable accuracy, and MAPE for PM<sub>2.5</sub> in all models is above 25 %, suggesting a relatively poor fit for predicting PM<sub>2.5</sub> concentrations. MASE is below 1 and indicates the model used in forecasting data shows forecasting performance was good.

In addition, R<sup>2</sup> yielded promising results for PM<sub>2.5</sub> prediction. The ARIMA model captured a moderate amount of variance (R<sup>2</sup> = 0.56), which means it explains a decent portion of the fluctuations in PM<sub>2.5</sub>

**Table 4**  
Predicted values of PM concentrations (µg/m<sup>3</sup>) in natural gas-fired power plants during 2022–2024.

ARIMA Forecasting													
	Year	Jan	Feb	Mar	Apr	May	Jun	July	Aug	Sep	Oct	Nov	Dec
PM <sub>2.5</sub>	2022	203.7	155.5	129.1	42.2	27.5	19.9	14.6	73.3	65.9	76.0	178.7	214.7
	2023	223.6	140.6	122.6	53.9	30.4	25.3	14.3	80.7	45.5	65.7	151.5	181.0
	2024	212.9	148.6	126.0	47.7	28.9	22.3	14.5	76.7	56.4	67.0	166.1	199.0
PM <sub>10</sub>	2022	364.5	302.5	297.0	201.7	160.0	139.5	111.6	207.3	215.2	270.6	323.6	337.5
	2023	391.1	336.7	313.5	200.4	150.3	118.1	89.5	205.4	213.6	274.9	333.9	354.3
	2024	391.3	325.2	306.4	209.6	152.7	127.2	87.5	205.8	189.0	246.7	315.7	332.7
ETS forecasting													
PM <sub>2.5</sub>	2022	191.0	149.3	110.4	40.5	30.1	20.8	14.7	41.3	41.9	45.0	98.3	157.3
	2023	191.0	149.3	110.4	40.5	30.1	20.8	14.7	41.3	42.0	45.0	98.3	157.3
	2024	149.3	110.4	40.5	30.1	20.8	14.7	41.3	40.0	45.0	98.3	157.3	199.0
PM <sub>10</sub>	2022	363.6	314.9	278.9	147.9	110.5	64.4	41.5	74.3	118.4	170.5	252.6	298.6
	2023	363.6	314.9	278.9	147.9	110.5	64.4	41.5	74.3	118.4	170.5	252.6	298.6
	2024	363.6	314.9	278.9	147.9	110.5	64.4	41.5	74.3	118.4	170.5	252.6	298.6
ANN forecasting													
PM <sub>2.5</sub>	2022	179.0	174.3	155.0	100.4	87.4	75.7	62.0	62.8	49.5	42.5	70.5	121.7
	2023	170.9	183.0	194.6	153.7	102.4	84.1	68.5	60.9	52.6	45.0	47.5	64.4
	2024	122.5	175.3	185.4	195.0	156.8	101.4	85.7	69.3	58.9	50.0	44.7	45.6
PM <sub>10</sub>	2022	367.8	366.8	365.0	245.0	233.3	219.6	150.8	126.0	111.7	119.8	219.9	237.9
	2023	269.1	345.1	367.6	265.0	232.0	137.2	121.0	110.8	105.7	106.1	124.4	123.9
	2024	170.9	238.1	269.1	290.3	234.5	220.2	136.5	111.7	104.9	103.6	106.5	107.0

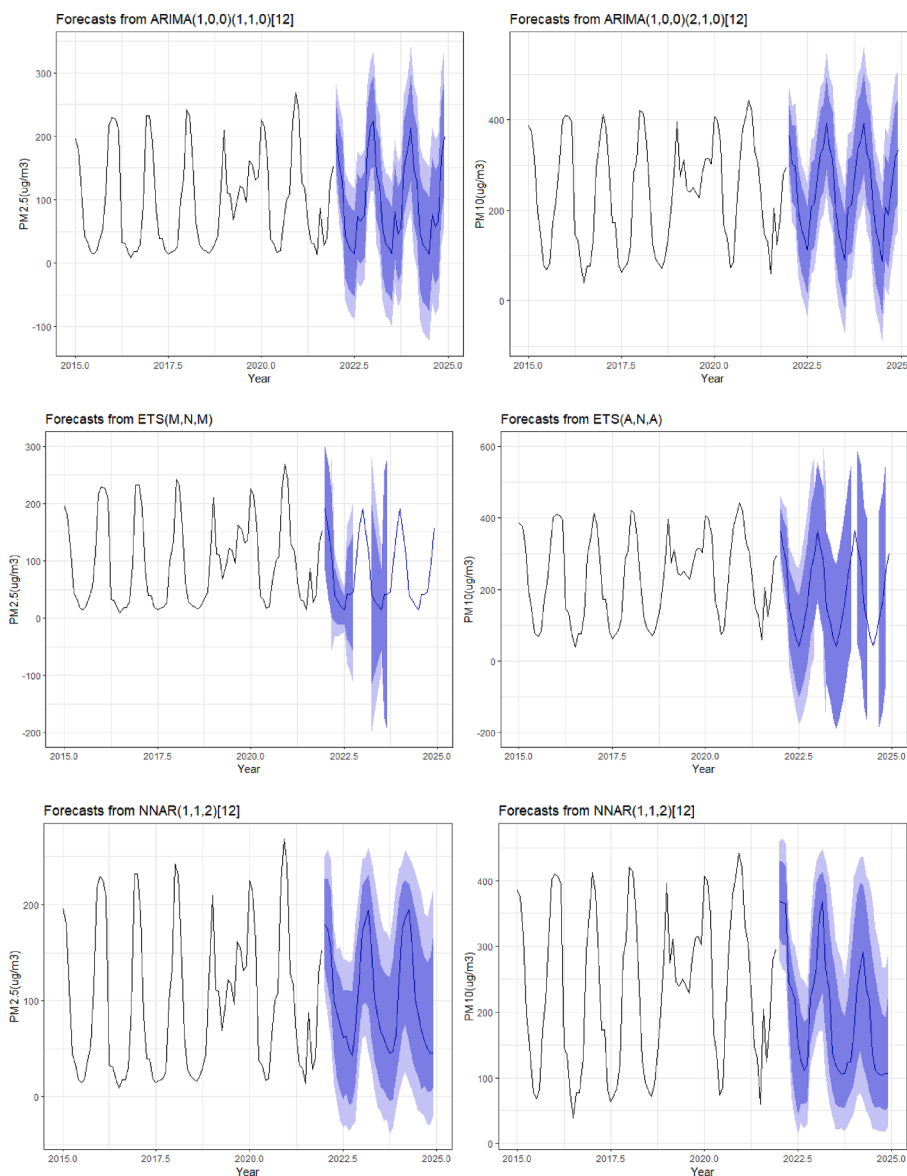


Fig. 3. Predicted vs. observed PM<sub>2.5</sub> and PM<sub>10</sub> values using ARIMA, ETS, and ANN models.

levels. The ETS model performed even better ( $R^2 = 0.64$ ), effectively capturing trends and seasonal patterns. The ANN model emerged as the leader ( $R^2 = 0.89$ ), explaining a very high proportion of the variance in PM<sub>2.5</sub> data. In statistical terms, an  $R^2$  of 1 indicates a perfect fit, while 0 signifies the model doesn't explain any variance. Therefore, the ANN model seems adept at capturing complex relationships in PM<sub>2.5</sub> data that other models might miss. However, PM<sub>10</sub> prediction remains a challenge. Both ARIMA and ETS models underperformed ( $R^2 < 0.06$ ), suggesting they may not be suitable for capturing the patterns in PM<sub>10</sub> concentrations. The ANN model also exhibited a negative  $R^2$ , indicating its forecasts were on average worse than simply using the historical average PM<sub>10</sub> value. Further investigation is necessary to identify a more effective model for PM<sub>10</sub> prediction.

### 3.4. Health impact assessment of particulate matter from natural gas-fired power plant

Electricity generation and fuel consumption are connected with air emissions from natural gas-fired power plants. Electricity utilities are regulated at the national level under DoE rules and regulations. Emissions from power plants pose a potentially considerable risk to human

health and the environment. These pollution sources are of particular concern in Bangladesh, where the burning of natural gas generates a large share of electricity. There are a variety of effects on human health depending on the content of air pollutants, the quantity, and duration of exposure, and the fact that people are often exposed to combinations of pollutants rather than single ones. Health consequences on people might include anything from cancer to nausea and respiratory problems. People working in a power plant exposed to emissions face health issues like breathing or skin irritation at a higher than the community people (Kampa and Castanas, 2008). Health effects can be distinguished into acute and chronic, not including cancer and cancerous. Epidemiological and animal model studies show that the cardiovascular and respiratory systems are predominantly impacted by the exposure (Pinkerton et al., 2019). Fig. 5 shows the yearly average air pollution level, including forecasted pollution mean level compared with AQI value and associated health risks in NG-fired power plants.

However, this research separated the year into four distinct seasons: winter (March-May), pre-monsoon (June-August), post-monsoon (September-November), and monsoon (December-February). Applying the ARIMA model to the data on PM<sub>2.5</sub>, it was predicted that during the monsoon season, natural gas-fired power plants will be

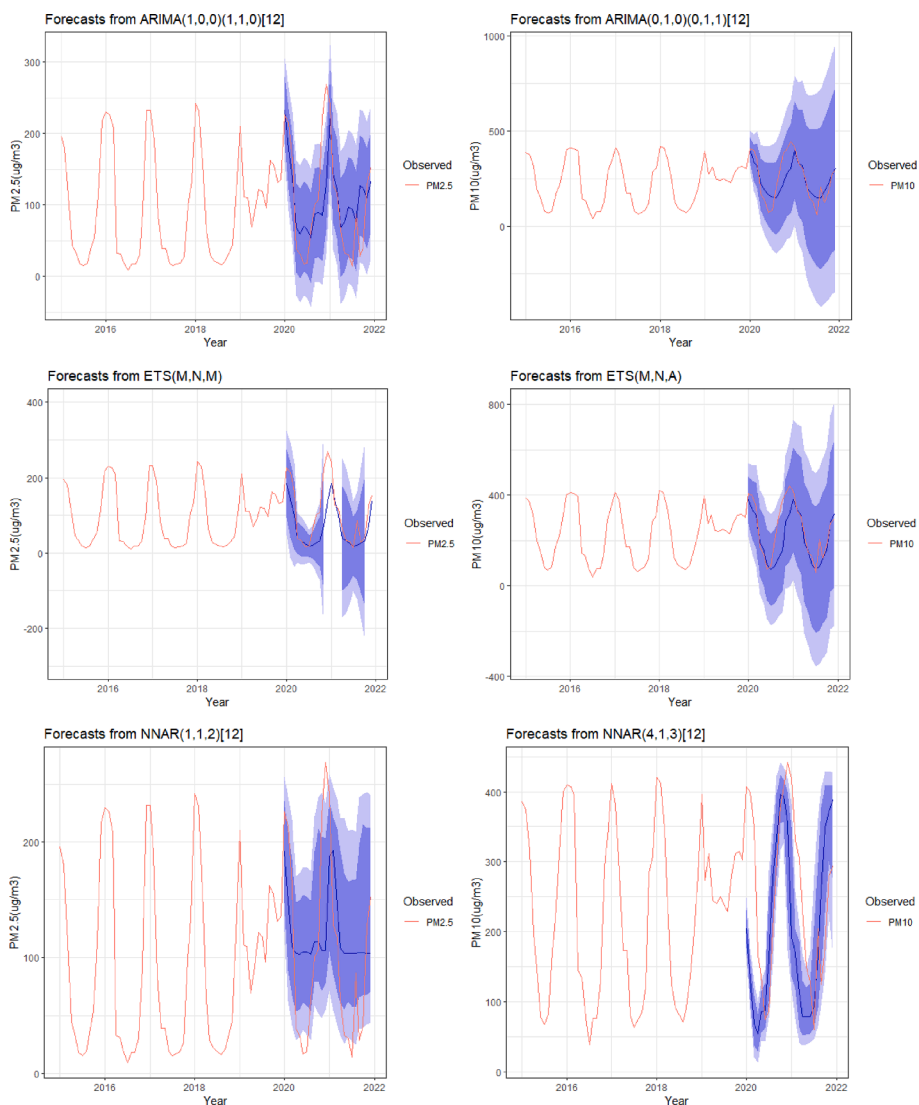


Fig. 4. Observed value vs. predicted value plot (accuracy of prediction).

Table 5

Error measure for the predicted value of ARIMA, ETS, and ANN models.

Models	Pollutants	RMSE	MAE	MAPE	MASE	R <sup>2</sup>
ARIMA	PM <sub>2.5</sub>	36.69	0.247	39.8	0.57	0.56
	PM <sub>10</sub>	48.49	0.363	20.26	0.59	0.062
ETS	PM <sub>2.5</sub>	49.07	0.306	38.25	0.70	0.64
	PM <sub>10</sub>	44.60	0.355	19.26	0.57	-0.10
ANN	PM <sub>2.5</sub>	36.63	0.283	45.94	0.65	0.89
	PM <sub>10</sub>	46.59	0.388	22.47	0.63	-0.01

N. B.: ARIMA = Auto-Regressive Integrated Moving Average, ETS = Error Trend Seasonal, ANN = Artificial Neural Network, RMSE = Root mean squared error, MAE = mean absolute error, MAPE = Mean absolute percentage error, MASE = mean absolute scaled error, R<sup>2</sup> = Coefficient of Determination.

unhealthy for sensitive groups in 2022, 2023, and 2024. The health hazard from PM<sub>10</sub> will be moderate in the 2024 monsoon season. ETS forecasting for 2022, 2023, and 2024 indicates that the health risk from PM<sub>2.5</sub> will be moderate in the monsoon season, and in the winter, the health risk will be very unhealthy in the power-generating site. According to the ANN forecasting model, due to PM<sub>2.5</sub>, health hazards will

be very unhealthy for the sensitive group in the pre-monsoon season of 2023 and 2024 and in the winter season of 2022 (Fig. 5). Digging deep into the health of natural gas-fired power plant workers, interviewed 100 employees. The results were alarming, 15 % reported grappling with health issues directly linked to the power plant’s air quality. This translated to 2 % struggling with respiratory problems and even higher 13 % bore the visible marks of poor air quality on their skin, with rashes and irritation a constant reminder of their occupational hazard. These statistics underscore the urgent need for stricter air quality regulations and better protective measures for power plant workers. However, implementing regular health checks, air filtration systems, and renewable energy consumption can provide a multitude of benefits for the environment. These practices promote healthier living, reduce environmental pollution, and contribute to a more sustainable future (Martínez-Mendoza et al., 2022).

#### 4. Conclusions

This study investigated PM<sub>2.5</sub> and PM<sub>10</sub> concentrations near natural gas-fired power plants using time series analysis and forecasting models ARIMA, ETS, and ANN to assess potential health risks associated with PM exposure and predict future air quality. Our findings revealed a link between PM concentrations and potential health problems like

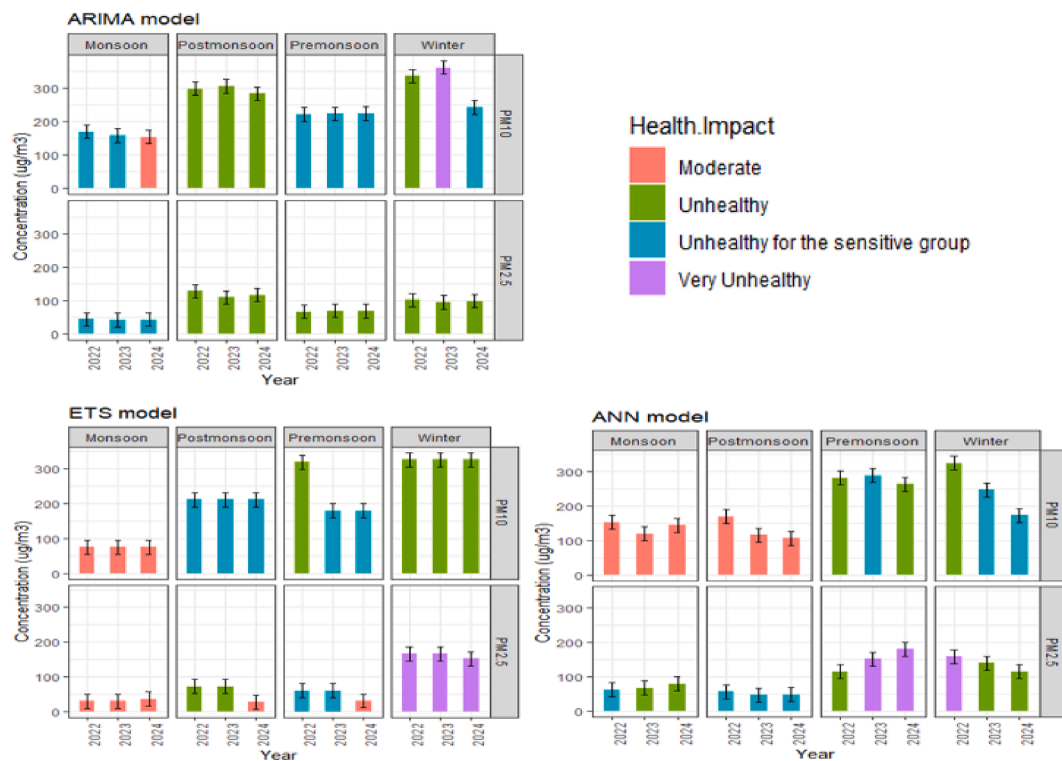


Fig. 5. The forecasted health impact of  $PM_{2.5}$  and  $PM_{10}$  concentration in natural gas power plants.

respiratory issues, heart disease, and premature death, aligning with established scientific evidence from the EPA. These results highlight the need for stricter PM control strategies to safeguard human health and environmental quality around these types of power plants.

## 5. Availability of data and material

The datasets used or analyzed during the current study are available from the first author upon reasonable request.

## Funding

This research was funded by the research grants of Research Cell, Noakhali Science and Technology University (No. NSTU/RC/MS/21/131).

## CRedit authorship contribution statement

**Mustafizur Rahman:** Writing – review & editing, Writing – original draft, Software, Methodology, Formal analysis, Data curation, Conceptualization. **Kamrul Hasan:** Visualization, Software, Formal analysis. **Md. Abu Bakar Siddique:** Writing – review & editing, Investigation. **Balram Ambade:** Writing – review & editing, Investigation. **Md. Alamgir Hussain:** Writing – review & editing. **Mohammed Abdus Salam:** Writing – review & editing, Supervision, Investigation, Funding acquisition. **Salman Tariq:** Writing – review & editing. **Muhammad Ibrahim:** Writing – review & editing.

## Declaration of competing interest

The authors declare that they have no known competing financial interests or personal relationships that could have appeared to influence the work reported in this paper.

## References

- Abdul Jameel, A.G., Elbaz, A.M., Emwas, A.H., Roberts, W.L., Sarathy, S.M., 2016. Calculation of average molecular parameters, functional groups, and a surrogate molecule for heavy fuel oils using  $1H$  and  $13C$  nuclear magnetic resonance spectroscopy. *Energy Fuels* 30, 3894–3905. <https://doi.org/10.1021/acs.energyfuels.6b00303>.
- Al-Amin, M., Sahabuddin, M., 2023. High penetration of electric autorickshaw on national power system and barriers against the adoption of solar energy: a case study in Bangladesh. *Clean Eng. Technol.* 14 <https://doi.org/10.1016/j.clet.2023.100637>.
- Anam, K., Husnain-Al-Bustam, 2011. Power crisis & its solution through renewable energy in bangladesh. *journal of selected areas in renewable and sustainable.* *Energy* 13–18.
- Bai, L., Wang, J., Ma, X., Lu, H., 2018. Air pollution forecasts: an overview. *Int. J. Environ. Res. Public Health.* <https://doi.org/10.3390/ijerph15040780>.
- BBS, SID, MoF, 2017. Bangladesh Statistics 2016. Bangladesh Bureau of Statistics Statistics and Informatics Division Ministry of Planning 73.
- Begum, B.A., Saroar, G., Nasiruddin, M., Randal, S., Sivertsen, B., Hopke, P.K., 2014a. Particulate Matter and Black Carbon Monitoring at Urban Environment in Bangladesh. *NUCLEAR SCIENCE AND APPLICATIONS* 23.
- Begum, B.A., Saroar, G., Nasiruddin, M., Randal, S., Sivertsen, B., Hopke, P.K., 2014b. Particulate matter and black carbon monitoring at urban environment in Bangladesh. *Nucl. Sci. Appl.* 23, 1–8.
- Cellura, M., Cusenza, M.A., Longo, S., 2018. Energy-related GHG emissions balances: IPCC versus LCA. *Sci. Total Environ.* 628–629, 1328–1339. <https://doi.org/10.1016/j.scitotenv.2018.02.145>.
- Cheng, W.L., Chen, Y.S., Zhang, J., Lyons, T.J., Pai, J.L., Chang, S.H., 2007. Comparison of the revised air quality index with the PSI and AQI indices. *Sci. Total Environ.* 382, 191–198. <https://doi.org/10.1016/j.scitotenv.2007.04.036>.
- Chowdhury, A.L., Uddin, M.J., Baul, T.K., Akhter, J., Nandi, R., Karmakar, S., Nath, T.K., 2022. Quantifying the potential contribution of urban trees to particulate matters removal: a study in Chattogram city, Bangladesh. *J. Clean. Prod.* 380, 135015 <https://doi.org/10.1016/j.jclepro.2022.135015>.
- Eğrioğlu, E., Aladağ, Ç.H., Günay, S., 2008. A new model selection strategy in artificial neural networks. *Appl. Math. Comput.* 195, 591–597. <https://doi.org/10.1016/j.amc.2007.05.005>.
- Ghenai, C., Bettayeb, M., 2021. Data analysis of the electricity generation mix for clean energy transition during COVID-19 lockdowns. *Energy Sources, Part A: Recovery, Utilization and Environmental Effects.* 10.1080/15567036.2021.1884772.
- Ghosh, S., 2002. Electricity consumption and economic growth in India. *Energy Policy* 30, 125–129.
- Gu, Y., Yan, F., Xu, J., Duan, Y., Fu, Q., Qu, Y., Liao, H., 2021. Mitigated  $PM_{2.5}$  Changes by the Regional Transport During the COVID-19 Lockdown in Shanghai, China. *Geophys. Res. Lett.* 48. 10.1029/2021GL092395.

- Holechek, J.L., Geli, H.M.E., Sawalhah, M.N., Valdez, R., 2022. A global assessment: can renewable energy replace fossil fuels by 2050? *Sustainability (Switzerland)* 14. <https://doi.org/10.3390/su14084792>.
- Ibe, F.C., Opara, A.I., Duru, C.E., Obinna, I.B., Enedoh, M.C., 2020. Statistical analysis of atmospheric pollutant concentrations in parts of Imo State, Southeastern Nigeria. *Sci. Afr.* 7 <https://doi.org/10.1016/j.sciaf.2019.e00237>.
- Islam, A., Ahmed, M.T., Mondal, M.A.H., Awual, M.R., Monir, M.U., Islam, K., 2021. A snapshot of coal-fired power generation in Bangladesh: a demand–supply outlook. *Nat. Resour. Forum.* 45, 157–182. <https://doi.org/10.1111/1477-8947.12221>.
- Islam, S., Khan, M.Z.R., 2017. A review of energy sector of bangladesh. *Energy Proc.* 110, 611–618. <https://doi.org/10.1016/j.egypro.2017.03.193>.
- Kampa, M., Castanas, E., 2008. Human health effects of air pollution. *Environ. Pollut.* <https://doi.org/10.1016/j.envpol.2007.06.012>.
- Kim, D., Han, H., Wang, W., Kang, Y., Lee, H., Kim, H.S., 2022. Application of deep learning models and network method for comprehensive air-quality index prediction. *Appl. Sci. (Switzerland)* 12. <https://doi.org/10.3390/app12136699>.
- Markandya, A., Wilkinson, P., 2007. Energy and Health 2 Electricity generation and health. *www.thelancet.com* 370. 10.1016/S0140.
- Martínez-Mendoza, E., Fernández-Echeverría, E., García-Santamaría, L.E., Ruvalcaba-Sánchez, L. and Fernández Lambert, G., 2022. Wind Farms Waste: Non-Calculated Environmental Impact?. Available at SSRN 4043654.
- Minh, V.T.T., Tin, T.T., Hien, T.T., 2021. PM2.5 forecast system by using machine learning and WRF Model, A Case Study: Ho Chi Minh City, Vietnam. *Aerosol. Air Qual. Res.* 21, 210108 <https://doi.org/10.4209/aaqr.210108>.
- Pinkerton, K.E., Chen, C.Y., Mack, S.M., Upadhyay, P., Wu, C.W., Yuan, W., 2019. Cardiopulmonary health effects of airborne particulate matter: correlating animal toxicology to human epidemiology. *Toxicol. Pathol.* 47, 954–961. <https://doi.org/10.1177/0192623319879091>.
- PSMP 2016, Power Division, Ministry of Power, Energy and Mineral Resources. Government of the People's Republic of Bangladesh.
- Qu, C.S., Ma, Z.W., Yang, J., Liu, Y., Bi, J., Huang, L., 2012. Human exposure pathways of heavy metals in a lead-zinc mining area, jiangsu province. *China. Plos One* 7. <https://doi.org/10.1371/journal.pone.0046793>.
- Radojević, D., Pocajt, V., Popović, I., Perić-Grujić, A., Ristić, M., 2013. Forecasting of greenhouse gas emissions in serbia using artificial neural networks. *Energy Sources, Part a: Recovery, Utilization and Environmental Effects* 35, 733–740. <https://doi.org/10.1080/15567036.2010.514597>.
- Rahman, M., Rashid, F., Roy, S.K., Habib, M.A., 2024. Application of extreme learning machine (ELM) forecasting model on CO2 emission dataset of a natural gas-fired power plant in Dhaka, Bangladesh. *Data Brief* 54, 110491. <https://doi.org/10.1016/j.dib.2024.110491>.
- Rashid, F., Joardder, M.U.H., 2022. Future options of electricity generation for sustainable development: trends and prospects. *Eng. Rep.* <https://doi.org/10.1002/eng2.12508>.
- Shahriar, S.A., Kayes, I., Hasan, K., Salam, M.A., Chowdhury, S., 2020. Applicability of machine learning in modeling of atmospheric particle pollution in Bangladesh. *Air Qual. Atmos. Health* 13, 1247–1256. <https://doi.org/10.1007/s11869-020-00878-8>.
- Shin, D., Kim, Y., Hong, K.J., Lee, G., Park, I., Kim, H.J., Kim, Y.J., Han, B., Hwang, J., 2022a. Measurement and Analysis of PM10 and PM2.5 from Chimneys of Coal-fired Power Plants Using a Light Scattering Method. *Aerosol Air Qual Res* 22. 10.4209/AAQR.210378.
- Shin, D., Kim, Y., Hong, K.J., Lee, G., Park, I., Kim, H.J., Kim, Y.J., Han, B., Hwang, J., 2022b. Measurement and Analysis of PM10 and PM2.5 from Chimneys of Coal-fired Power Plants Using a Light Scattering Method. *Aerosol Air Qual Res* 22. 10.4209/AAQR.210378.
- Sokulski, C.C., Barros, M.V., Salvador, R., Broday, E.E., de Francisco, A.C., 2022. Trends in renewable electricity generation in the g20 countries: an analysis of the 1990–2020 period. *Sustainability (switzerland)* 14. <https://doi.org/10.3390/su14042084>.
- Thabani, N., Wellington, G., Bonga, 2019. Prediction of Emissions in India using ARIMA Models. *DRJ J. Econ. Finance*.
- Vultaggio, M., Varrica, D., Alaimo, M.G., 2020. Impact on air quality of the COVID-19 lockdown in the urban area of palermo (Italy). *Int. J. Environ. Res. Public Health* 17, 7375. <https://doi.org/10.3390/ijerph17207375>.
- Wang, W., Lu, Y., 2018. In: Analysis of the Mean Absolute Error (MAE) and the Root Mean Square Error (RMSE) in Assessing Rounding Model. Institute of Physics Publishing. <https://doi.org/10.1088/1757-899X/324/1/012049>.
- Woodward, A., Smith, K.R., Campbell-Lendrum, D., Chadee, D.D., Honda, Y., Liu, Q., Olwoch, J., Revich, B., Sauerborn, R., Chafe, Z., Confalonieri, U., Haines, A., 2014. Climate change and health: On the latest IPCC report. *The Lancet.* [https://doi.org/10.1016/S0140-6736\(14\)60576-6](https://doi.org/10.1016/S0140-6736(14)60576-6).